# OPTIMUM LENGTH OF A ROCKET-WALL EXTENSION BEYOND ITS CIRCUMFERENTIAL KEYWAY*

Bernard W. Shaffer

*Department of Mechanical Engineering, New York University, New York, N. Y.*

Ira Cochin

*Kearfott Co., Inc., Clifton, N. J.*

Morton Mantus

*Grumman Aircraft Engineering Corp., Bethpage, N. Y.*

## *Introduction*

One of the common closure arrangements found in rocket design is shown diagrammatically in FIGURE 1. The outside diameter of the rocket is constant and the wall thickness remains uniform for a considerable length of the unit. A short distance from the end, however, the cylinder is recessed to accommodate a circumferential key that connects the rocket wall to an end closure that maintains internal pressure within the assembly.

The relatively short section of the rocket wall that extends beyond the keyway serves primarily to retain the key but, in addition, it makes some contribution to the stiffness of the structure. The exact contribution obviously depends on the length of the extension, with longer sections contributing greater stiffness. One may expect, however, that there exists some optimum length beyond which there results very little increase in the length of the extension. Since weight savings are an important consideration in rocket design, the current study was conducted with the objective of determining the optimum distance from the keyway to the edge of the vessel, so that maximum stiffness is developed at the recessed section while utilizing a minimum amount of material.

The study of the rocket-wall problem is based on discontinuity theory. According to this theory, a structure under investigation is hypothetically separated into a number of free bodies at sections where discontinuity of loading, material, or cross section is present. Each of the resulting free bodies is then studied under the influence of the externally applied

*This paper, illustrated with slides, was presented at a meeting of the Division of Engineering on January 16, 1959. The results presented in this article were obtained in the course of research sponsored by the Bureau of Ordnance, Department of the Navy, Washington, D.C., under Contract No. NOrd-16497, with New York University.

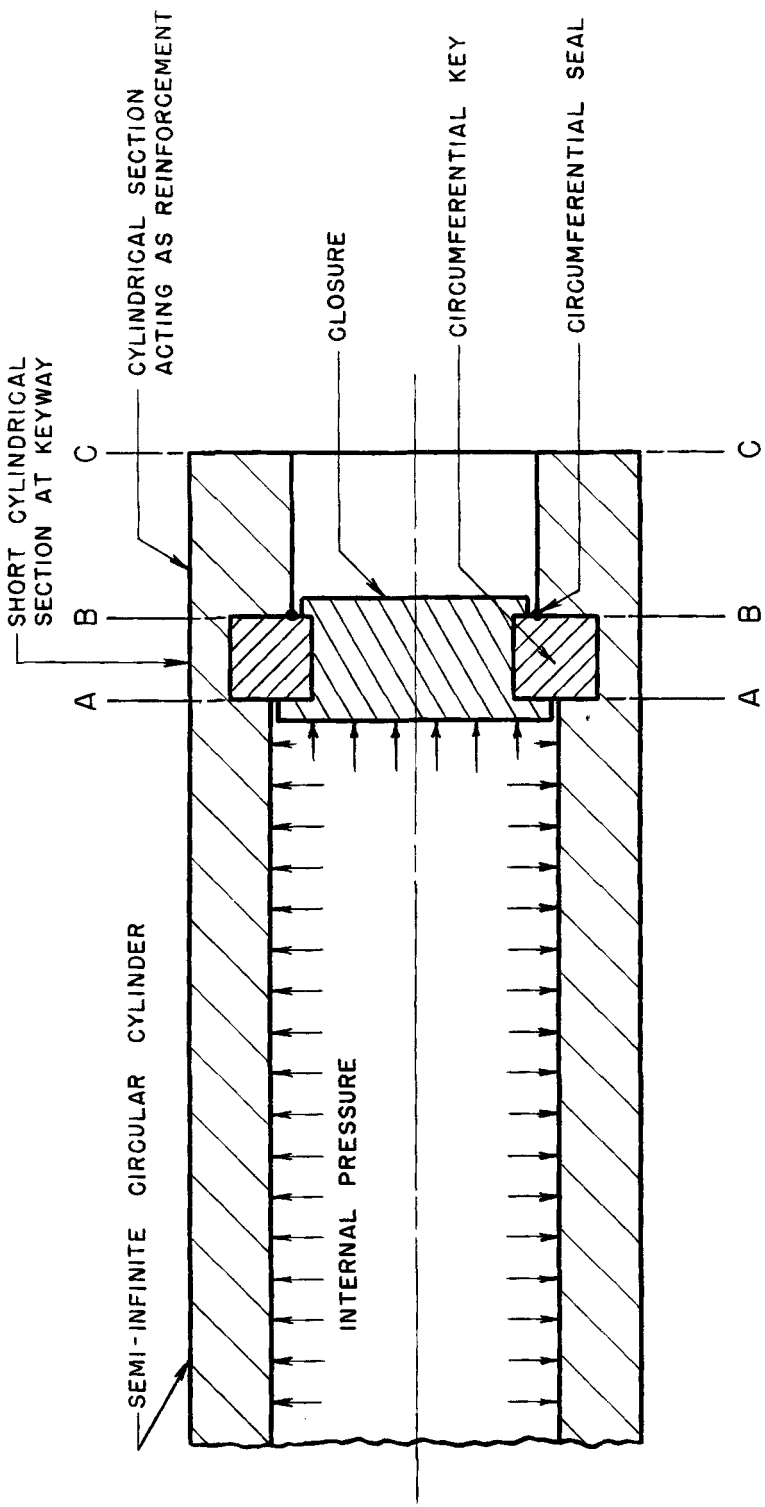


FIGURE 1. The circular semi-infinite rocket wall containing a circumferential keyway. Not drawn to scale.

loads, as well as the resultant bending moments, shear forces, and tensile forces that must be introduced to represent the stress system as it existed before the original structure was subdivided. The resultant moments and forces appear initially as unknown quantities, but may be evaluated subsequently by imposing the requirement of continuity of deformation at the junctions.

In most rockets, the wall thickness is sufficiently small in comparison to its mean radius to make possible the use of shell theory in analyzing each of the free bodies. Shell theory was also applicable in analyzing sections of other composite structures previously studied by Watts and Lang,[1] Watts and Burrows,[2] McCalley and Kelly,[3] and Horvay and Clausen,[4,5] to name a few. In each case these investigators also employed discontinuity techniques.

Although solutions to shell theory problems appear in the literature, they are not always complete, nor are they in a form suitable for the present study. Consequently, in order to present the rocket study from a unified and consistent point of view, the solutions to the general problem of deformation of a thin-walled circular cylinder subjected to an arbitrary system of axially symmetrical forces is included in this paper. Since the solution to the general problem contains parameters that are complicated functions of the geometry, tables of these constants are included.

### *Analysis of a Short Circular Cylinder*

FIGURE 2 shows a cylinder of length $\ell$, subjected to internal pressure $p$, axial tensile forces $H$ and $T$, bending moments $M_R$ and $M_L$, and shearing forces $Q_R$ and $Q_L$, all defined positive as shown. The foregoing moments and forces are loads per unit length, and are assumed to be uniformly distributed around the circumference; the subscripts $R$ and $L$ refer to the right and left edges of the cylinder, respectively. The positive directions were chosen as shown in FIGURE 2, so that the same sign convention may be used for two adjacent bodies, thus permitting simple and systematic writing of continuity equations at the surface of separation.

Two axial forces, $H$ and $T$, are shown acting on the section to distinguish two different effects. The axial force $H$ is caused by the internal pressure within the cylinder, while $T$ is the axial force induced by any external system of loads. If the cylinder is closed at both ends and subjected to internal pressure $p$, the resultant force on the end closure is transmitted through the cylinder as an axial force $H$ equal to $pR/2$. Should the cylinder not be closed at both ends, $H$ is obviously zero. Since $T$ depends on an external system of loads, its magnitude depends on the application.

FIGURE 3 shows the sign conventions selected for the deformations at the end of the cylinder. The radial displacement $w$ is taken positive at either end when it is radially inward. Rotation $\theta_L$ at the left end of the

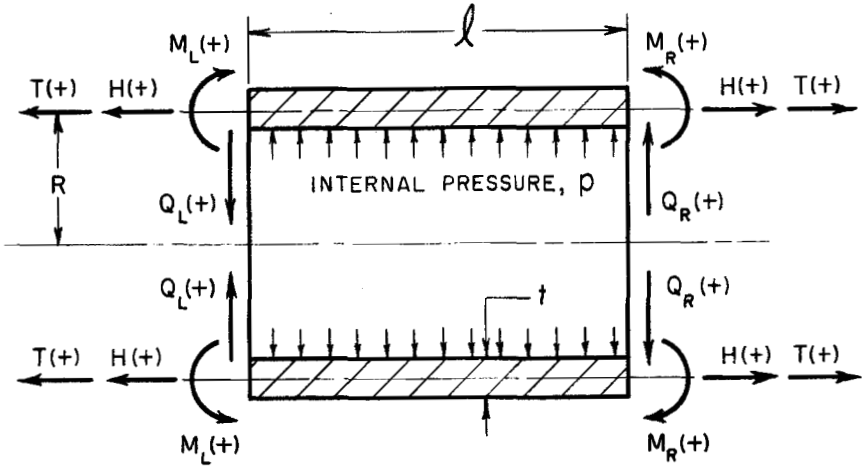


FIGURE 2. The sign convention for the forces on a short circular cylinder.

cylinder is taken as positive if it is toward the axis, while rotation $\theta_R$ at the right end of the cylinder is taken positive if it is away from its axis.

It can be shown[6] that when $H$ and $T$ are equal to zero, the radial displacement $w$ of the circular cylinder shown in FIGURE 2 satisfies the differential equation

$$d^4w/dx^4 + 4\beta^4 w = -p/D \tag{1}$$

where

$$\beta^4 = 3(1 - \mu^2)/R^2t^2; \quad D = Et^3/12\,(1 - \mu^2) \tag{2}$$

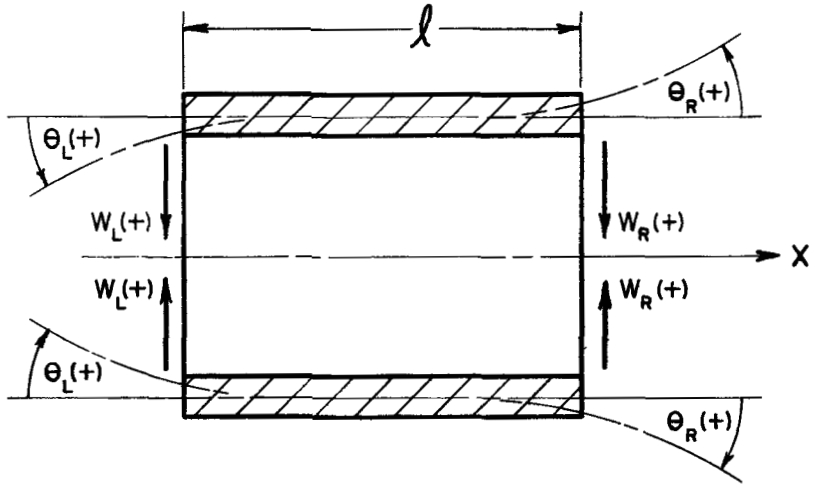


FIGURE 3. The sign convention for the deformation of a short circular cylinder.

and $p$ denotes the internal pressure, $E$ is the modulus of elasticity, $\mu$ is Poisson's ratio, $R$ is the mean radius, and $t$ is the wall thickness of the cylinder. $D$ is usually referred to as the flexural rigidity.

The solution to EQUATION 1 may be expressed as

$$w = e^{\beta x}(C_1 \cos \beta x + C_2 \sin \beta x) + e^{-\beta x}(C_3 \cos \beta x + C_4 \sin \beta x) - R^2 p/Et \quad (3)$$

The four constants $C_1$, $C_2$, $C_3$, and $C_4$ may be evaluated in the terms of the bending moments and shearing forces that exist at the ends of the cylinder by using the relations between the radial displacement $w$ and the forces on the boundary, namely

$$[M_x]_{x=0} = -D[d^2w/dx^2]_{x=0} = M_L\,;\ [Q_x]_{x=0} = -D[d^3w/dx^3]_{x=0} = -Q_L$$
$$[M_x]_{x=\ell} = -D[d^2w/dx^2]_{x=\ell} = M_R\,;\ [Q_x]_{x=\ell} = -D[d^3w/dx^3]_{x=\ell} = -Q_R \quad (4)$$

Application of these expressions to EQUATION 3 leads to the following equations for deflection $w$ and rotation $\theta = dw/dx$ at the left and right edges of the cylinder:

$$\theta_L = -(S/2\beta D)M_L + (B/2\beta^2 D)Q_L + (Y/2\beta D)M_R + (K/2\beta^2 D)Q_R \quad (5)$$

$$w_L = -(B/2\beta^2 D)M_L + (L/2\beta^3 D)Q_L + (K/2\beta^2 D)M_R + V/2\beta^3 D)Q_R - pR^2/Et \quad (6)$$

$$\theta_R = -(Y/2\beta D)M_L + (K/2\beta^2 D)Q_L + (S/2\beta D)M_R + (B/2\beta^2 D)Q_R \quad (7)$$

$$w_R = (K/2\beta^2 D)M_L - (V/2\beta^3 D)Q_L - (B/2\beta^2 D)M_R - (L/2\beta^3 D)Q_R - pR^2/Et \quad (8)$$

where the parameters $K$, $B$, $S$, $Y$, $L$ and $V$* are defined as follows:

$$\begin{aligned}
(\mathrm{Sinh}^2\,\beta\ell - \sin^2\beta\ell)\,K &= 2\sin\beta\ell\,\mathrm{Sinh}\,\beta\ell\\
(\mathrm{Sinh}^2\,\beta\ell - \sin^2\beta\ell)\,B &= \mathrm{Sinh}^2\,\beta\ell + \sin^2\beta\ell\\
(\mathrm{Sinh}^2\,\beta\ell - \sin^2\beta\ell)\,S &= 2\sin\beta\ell\cos\beta\ell + 2\,\mathrm{Sinh}\,\beta\ell\,\mathrm{Cosh}\,\beta\ell\\
(\mathrm{Sinh}^2\,\beta\ell - \sin^2\beta\ell)\,Y &= 2\sin\beta\ell\,\mathrm{Cosh}\,\beta\ell + 2\cos\beta\ell\,\mathrm{Sinh}\,\beta\ell\\
(\mathrm{Sinh}^2\,\beta\ell - \sin^2\beta\ell)\,L &= \mathrm{Sinh}\,\beta\ell\,\mathrm{Cosh}\,\beta\ell - \sin\beta\ell\cos\beta\ell\\
(\mathrm{Sinh}^2\,\beta\ell - \sin^2\beta\ell)\,V &= \sin\beta\ell\,\mathrm{Cosh}\,\beta\ell - \cos\beta\ell\,\mathrm{Sinh}\,\beta\ell
\end{aligned} \quad (9)$$

*The scientific staff of M. W. Kellogg Company is responsible for the original definition of these parameters and for the preparation of TABLE 1. Their original work appears in an unpublished report.[7]

These terms act as influence coefficients for the cylinder. For convenience, their numerical values are given in TABLE 1 for values of $\beta\ell$ from 0.5 to 5.0.

TABLE 1

| $\beta\ell$ | $K$ | $B$ | $S$ | $Y$ | $L$ | $V$ |
|---|---|---|---|---|---|---|
| 0.50 | 12.00 | 12.00 | 46.60 | 46.10 | 4.00 | 2.000 |
| 0.60 | 8.31 | 8.37 | 27.70 | 27.10 | 3.33 | 1.670 |
| 0.70 | 6.09 | 6.17 | 18.10 | 17.40 | 2.87 | 1.430 |
| 0.80 | 4.65 | 4.76 | 12.40 | 11.60 | 2.51 | 1.240 |
| 0.90 | 3.65 | 3.78 | 8.89 | 7.99 | 2.23 | 1.100 |
| 1.00 | 2.94 | 3.10 | 6.74 | 5.75 | 2.02 | 0.986 |
| 1.10 | 2.41 | 2.61 | 5.32 | 4.23 | 1.85 | 0.890 |
| 1.20 | 1.99 | 2.23 | 4.35 | 3.17 | 1.70 | 0.809 |
| 1.30 | 1.68 | 1.95 | 3.69 | 2.41 | 1.58 | 0.738 |
| 1.40 | 1.41 | 1.73 | 3.22 | 1.84 | 1.48 | 0.676 |
| 1.50 | 1.20 | 1.56 | 2.87 | 1.41 | 1.39 | 0.621 |
| 1.60 | 1.02 | 1.43 | 2.61 | 1.08 | 1.32 | 0.570 |
| 1.70 | 0.875 | 1.33 | 2.44 | 0.821 | 1.27 | 0.523 |
| 1.80 | 0.745 | 1.24 | 2.31 | 0.616 | 1.21 | 0.480 |
| 1.90 | 0.632 | 1.18 | 2.22 | 0.445 | 1.17 | 0.438 |
| 2.00 | 0.535 | 1.13 | 2.15 | 0.310 | 1.14 | 0.400 |
| 2.10 | 0.450 | 1.10 | 2.10 | 0.201 | 1.11 | 0.363 |
| 2.20 | 0.375 | 1.07 | 2.07 | 0.111 | 1.09 | 0.329 |
| 2.30 | 0.309 | 1.05 | 2.05 | 0.0392 | 1.07 | 0.296 |
| 2.40 | 0.251 | 1.03 | 2.03 | −0.0188 | 1.05 | 0.265 |
| 2.50 | 0.200 | 1.02 | 2.02 | −0.0649 | 1.04 | 0.235 |
| 2.60 | 0.155 | 1.01 | 2.01 | −0.101 | 1.03 | 0.207 |
| 2.70 | 0.116 | 1.01 | 2.01 | −0.128 | 1.02 | 0.181 |
| 2.80 | 0.0819 | 1.00 | 2.01 | −0.148 | 1.01 | 0.157 |
| 2.90 | 0.0529 | 1.00 | 2.01 | −0.161 | 1.01 | 0.134 |
| 3.00 | 0.0282 | 1.00 | 2.01 | −0.169 | 1.01 | 0.113 |
| 3.10 | 0.00751 | 1.00 | 2.01 | −0.173 | 1.00 | 0.0940 |
| 3.20 | −0.00953 | 1.00 | 2.01 | −0.173 | 1.00 | 0.0767 |
| 3.30 | −0.0233 | 1.00 | 2.01 | −0.169 | 1.00 | 0.0613 |
| 3.40 | −0.0342 | 1.00 | 2.01 | −0.163 | 1.00 | 0.0475 |
| 3.50 | −0.0424 | 1.00 | 2.01 | −0.156 | 1.00 | 0.0354 |
| 3.60 | −0.0484 | 1.00 | 2.01 | −0.147 | 1.00 | 0.0248 |
| 3.70 | −0.0525 | 1.00 | 2.01 | −0.137 | 1.00 | 0.0157 |
| 3.80 | −0.0548 | 1.00 | 2.01 | −0.126 | 1.00 | 0.00800 |
| 3.90 | −0.0558 | 1.00 | 2.01 | −0.115 | 1.00 | 0.00152 |
| 4.00 | −0.0555 | 1.00 | 2.00 | −0.103 | 1.00 | −0.00380 |
| 4.10 | −0.0543 | 1.00 | 2.00 | −0.0925 | 1.00 | −0.00809 |
| 4.20 | −0.0523 | 1.00 | 2.00 | −0.0818 | 1.00 | −0.0115 |
| 4.30 | −0.0498 | 1.00 | 2.00 | −0.0716 | 1.00 | −0.0140 |
| 4.40 | −0.0468 | 1.00 | 2.00 | −0.0619 | 1.00 | −0.0158 |
| 4.50 | −0.0435 | 1.00 | 2.00 | −0.0528 | 1.00 | −0.0171 |
| 4.60 | −0.0400 | 1.00 | 2.00 | −0.0445 | 1.00 | −0.0177 |
| 4.70 | −0.0364 | 1.00 | 2.00 | −0.0369 | 1.00 | −0.0180 |
| 4.80 | −0.0328 | 1.00 | 2.00 | −0.0299 | 1.00 | −0.0178 |
| 4.90 | −0.0293 | 1.00 | 2.00 | −0.0237 | 1.00 | −0.0174 |
| 5.00 | −0.0259 | 1.00 | 2.00 | −0.0182 | 1.00 | −0.0167 |

If, on the other hand, the axial forces $H$ and $T$ have nonzero values, an additional radial deflection occurs due to the Poisson effect and is given by

$$w = \mu HR/Et + \mu TR/Et \tag{10}$$

Thus, for a pressurized vessel with closed ends, the deflections at the ends of the cylinder may be found by substituting EQUATIONS 10 and $H = pR/2$ into EQUATIONS 6 and 8, to obtain

$$w_L = -\frac{B}{2\beta^2 D} M_L + \frac{L}{2\beta^3 D} Q_L + \frac{K}{2\beta^2 D} M_R + \frac{}{2\beta^3 D} Q_R - (1 - \frac{\mu}{2}) \frac{pR^2}{Et} + \frac{\mu TR}{Et} \tag{11}$$

$$w_R = \frac{K}{2\beta^2 D} M_L - \frac{V}{2\beta^3 D} Q_L - \frac{B}{2\beta^2 D} M_R - \frac{L}{2\beta^3 D} Q_R - (1 - \frac{\mu}{2}) \frac{pR^2}{Et} + \frac{\mu TR}{Et} \tag{12}$$

The corresponding rotations, as given in EQUATIONS 5 and 7, remain unaltered.

In numerical computations based on the foregoing deformation equations, it is convenient to combine the parameters defined in EQUATIONS 2 in the following manner:

$$\beta D = Et^2/a\rho^{1/2}; \quad 2\beta D = Et^2/b\rho^{1/2}$$
$$2\beta^2 D = Et/c\rho; \quad 2\beta^3 D = E/d\rho^{3/2} \tag{13}$$

where

$$\rho = R/t \tag{14}$$

$$[3(1 - \mu^2)]^{1/4} a = 12(1 - \mu^2); \qquad [3(1 - \mu^2)]^{1/2} c = 6(1 - \mu^2)$$
$$[3(1 - \mu^2)]^{1/4} b = 6(1 - \mu^2); \qquad [3(1 - \mu^2)]^{3/4} d = 6(1 - \mu^2) \tag{15}$$

The expressions for $a$, $b$, c and $d$ are functions of only Poisson's ratio $\mu$, and hence may be treated as constants in most problems. For convenience, their values, as well as the coefficient $(1 - \mu/2)$, are presented in TABLE 2 for a range of $\mu$ from 0.25 to 0.50.

After introducing EQUATIONS 13 into EQUATIONS 5, 11, 7, and 12, the deformation equations may be rewritten in terms of the newly defined dimensionless quantities, to read

$$\theta_L = -bS\frac{\rho^{1/2}}{Et^2}M_L + cB\frac{\rho}{Et}Q_L + bY\frac{\rho^{1/2}}{Et^2}M_R + cK\frac{\rho}{Et}Q_R \tag{16}$$

$$w_L = -cB\frac{\rho}{Et}M_L + dL\frac{\rho^{3/2}}{E}Q_L + cK\frac{\rho}{Et}M_R + dV\frac{\rho^{3/2}}{E}Q_R - (1-\frac{\mu}{2})\frac{pR^2}{Et} + \frac{\mu TR}{Et} \tag{17}$$

$$\theta_R = -bY\frac{\rho^{1/2}}{Et^2}M_L + cK\frac{\rho}{Et}Q_L + bS\frac{\rho^{1/2}}{Et^2}M_R + cB\frac{\rho}{Et}Q_R \tag{18}$$

$$w_R = cK\frac{\rho}{Et}M_L - dV\frac{\rho^{3/2}}{E}Q_L - cB\frac{\rho}{Et}M_R - dL\frac{\rho^{3/2}}{E}Q_R - (1-\frac{\mu}{2})\frac{pR^2}{Et} + \frac{\mu TR}{Et} \tag{19}$$

The equations mathematically represent the deflections and rotations at the ends of a circular cylinder subject to axially symmetrical loading. Two special cases are of particular interest in the analysis to follow. These are the limiting cases when $\beta\ell \to 0$ and when $\beta\ell \to \infty$. As $\beta\ell \to 0$, a cylinder becomes sufficiently short so that, under load, there is essentially no difference in the rotation of the two ends. This limiting case is called the circular ring. The second case, termed the semi-infinite cylinder, is evolved when $\beta\ell \to \infty$. In this case the cylinder is so long that a load applied at one end has no appreciable effect on the deformation at the other end. These special cases are considered in the next two sections.

### *The Circular Cylindrical Ring*

In the previous section, expressions were developed for deflections and rotations at the ends of a short circular cylinder subjected to an arbitrary system of loads. These expressions were written in terms of the influence coefficients $K$, $B$, $S$, $Y$, $L$, and $V$ described in EQUATIONS 9. Expansion in series form of the trigonometric and hyperbolic functions used to describe the influence coefficients permits the rewriting of EQUATIONS 9 as

$$K = \frac{3}{(\beta\ell)^2}\left[1 - \frac{1}{90}(\beta\ell)^4 + \ldots\right]; \quad Y = \frac{6}{(\beta\ell)^3}\left[1 - \frac{1}{30}(\beta\ell)^4 + \ldots\right]$$

$$B = \frac{3}{(\beta\ell)^2}\left[1 + \frac{2}{45}(\beta\ell)^4 + \ldots\right]; \quad L = \frac{2}{\beta\ell}\left[1 + \frac{2}{105}(\beta\ell)^4 + \ldots\right] \tag{20}$$

$$S = \frac{6}{(\beta\ell)^3}\left[1 + \frac{2}{15}(\beta\ell)^4 + \ldots\right]; \quad V = \frac{1}{\beta\ell}\left[1 - \frac{1}{210}(\beta\ell)^4 + \ldots\right]$$

For small values of $\beta\ell$ the terms of higher order may be neglected, and the influence coefficients become simply

$$K = B = \frac{3}{(\beta\ell)^2}\ ;\ S = Y = \frac{6}{(\beta\ell)^3}\ ;\ L = \frac{2}{\beta\ell}\ ;\ V = \frac{1}{\beta\ell} \qquad (21)$$

Comparison of EQUATIONS 20 and 21 shows that it is reasonable to drop the terms of higher order whenever $\beta\ell < 0.5$, since the error introduced in the numerical values of the influence coefficients is then very small.

It may thus be concluded that, when the value of the parameter $\beta\ell$ for a circular cylinder is less than 0.5, its influence coefficients may be evaluated from EQUATIONS 21. A cylinder of this type may then be called a circular cylindrical ring. The deformations of the ring are still given by EQUATIONS 16, 17, 18, and 19.

TABLE 2

| $\mu$ | $a$ | $b$ | $c$ | $d$ | $(1-\frac{\mu}{2})$ |
|---|---|---|---|---|---|
| 0.25 | 8.6873 | 4.3437 | 3.3542 | 2.5901 | 0.875 |
| 0.26 | 8.6514 | 4.3257 | 3.3449 | 2.5864 | 0.870 |
| 0.27 | 8.6148 | 4.3074 | 3.3355 | 2.5828 | 0.865 |
| 0.28 | 8.5763 | 4.2882 | 3.3255 | 2.5789 | 0.860 |
| 0.29 | 8.5365 | 4.2683 | 3.3153 | 2.5749 | 0.855 |
| 0.30 | 8.4981 | 4.2490 | 3.3066 | 2.5732 | 0.850 |
| 0.31 | 8.4529 | 4.2265 | 3.2935 | 2.5667 | 0.845 |
| 0.32 | 8.4084 | 4.2042 | 3.2819 | 2.5620 | 0.840 |
| 0.33 | 8.3626 | 4.1813 | 3.2701 | 2.5573 | 0.835 |
| 0.34 | 8.3153 | 4.1577 | 3.2577 | 2.5524 | 0.830 |
| 0.35 | 8.2666 | 4.1333 | 3.2450 | 2.5475 | 0.825 |
| 0.36 | 8.2165 | 4.1083 | 3.2319 | 2.5424 | 0.820 |
| 0.37 | 8.1649 | 4.0825 | 3.2183 | 2.5372 | 0.815 |
| 0.38 | 8.1119 | 4.0560 | 3.2043 | 2.5316 | 0.810 |
| 0.39 | 8.0567 | 4.0284 | 3.1898 | 2.5258 | 0.805 |
| 0.40 | 8.0006 | 4.0003 | 3.1750 | 2.5200 | 0.800 |
| 0.41 | 7.9424 | 3.9712 | 3.1595 | 2.5137 | 0.795 |
| 0.42 | 7.8826 | 3.9413 | 3.1437 | 2.5074 | 0.790 |
| 0.43 | 7.8218 | 3.9109 | 3.1276 | 2.5011 | 0.785 |
| 0.44 | 7.7588 | 3.8794 | 3.1107 | 2.4941 | 0.780 |
| 0.45 | 7.6948 | 3.8474 | 3.0935 | 2.4873 | 0.775 |
| 0.46 | 7.6291 | 3.8146 | 3.0759 | 2.4804 | 0.770 |
| 0.47 | 7.5616 | 3.7808 | 3.0577 | 2.4731 | 0.765 |
| 0.48 | 7.4918 | 3.7459 | 3.0389 | 2.4652 | 0.760 |
| 0.49 | 7.4209 | 3.7105 | 3.0195 | 2.4572 | 0.755 |
| 0.50 | 7.3487 | 3.6744 | 3.0000 | 2.4495 | 0.750 |

*The Semi-Infinite Circular Cylinder*

Another special case of the short circular cylinder that is of considerable importance in practical problems is the semi-infinite cylinder. It may be observed by examining EQUATIONS 9 that, as $\beta\ell$ increases indefinitely, the influence coefficients approach the following limiting values:

$$\begin{aligned} &\lim_{\beta\ell \to \infty} K = 0; \quad \lim_{\beta\ell \to \infty} S = 2.00; \quad \lim_{\beta\ell \to \infty} L = 1.00 \\ &\lim_{\beta\ell \to \infty} B = 1.00; \quad \lim_{\beta\ell \to \infty} Y = 0; \quad \lim_{\beta\ell \to \infty} V = 0 \end{aligned} \tag{22}$$

A comparison of the values of the influence coefficients as given by EQUATIONS 22 with those listed in TABLE 1 indicates that the limiting values may be used in the practical analysis of cylinders whenever $\beta\ell > 5.0$ without introducing appreciable error.

The deflection and rotation at the right edge of a pressurized semi-infinite cylinder loaded at the right edge with bending moment, shear, and axial load are given by EQUATIONS 19 and 18 with influence coefficients defined in EQUATIONS 22. Thus

$$w_R = -c\frac{\rho}{Et}M_R - d\frac{\rho^{3/2}}{E}Q_R - (1-\frac{\mu}{2})\frac{pR^2}{Et} + \frac{\mu TR}{Et} \tag{23a}$$

$$\theta_R = a\frac{\rho^{1/2}}{Et^2}M_R + c\frac{\rho}{Et}Q_R \tag{23b}$$

Similarly, in view of EQUATIONS 17, 16, and 22, the deformations at the left edge of a semi-infinite cylinder due to loads at the corresponding edge are given by

$$w_L = -c\frac{\rho}{Et}M_L + d\frac{\rho^{3/2}}{E}Q_L - (1-\frac{\mu}{2})\frac{pR^2}{Et} + \frac{\mu TR}{Et} \tag{24a}$$

$$\theta_L = -a\frac{\rho^{1/2}}{Et^2}M_L + c\frac{\rho}{Et}Q_L \tag{24b}$$

The coefficients $\rho$, $a$, $b$, $c$, and $d$ retain their original definitions given in EQUATIONS 14 and 15.

In summary, then, the analysis of deflections and rotations of all thin-walled, circular cylinders subjected to axially symmetrical loads may be placed into one of the following three categories:

(1) If $0 < \beta\ell < 0.5$ for a given cylinder, it may be treated as a circular cylindrical ring. The simplified coefficients given in EQUATIONS 21 may

then be used in conjunction with EQUATIONS 16, 17, 18, and 19 to obtain the deflections and rotations.

(2) If, however, for a given cylinder, $0.5 \leq \beta\ell \leq 5.0$, then EQUATIONS 16, 17, 18, and 19 still apply, but the influence coefficients are defined in EQUATIONS 19 and are listed in TABLE 1.

(3) For relatively long cylinders, $\beta\ell > 5.0$, one may use the semi-infinite cylinder approximation with reasonable accuracy. In this case, the deflections and rotations may be calculated by using EQUATIONS 23 or 24.

*Analysis of the Recessed, Semi-Infinite Cylinder*

Consider the problem of the cylinder recessed to retain a circumferential key as shown in FIGURE 1. To study the effect of the length of the wall that extends beyond the keyway on the stiffness of the structure, it is desirable to express the deformation at Section *B-B* in terms of the other parameters of the cylinder, since this deformation may be used as a convenient measure of stiffness.

The effect of internal pressure acting on the end closure is included in the deformation study by introducing a force per unit length $F$ equal to the resultant force on the closure and uniformly distributed around the keyway. The rocket may then be analyzed as a recessed circular cylinder under the influence of the force $F$ and the internal pressure $p$.

In conformity with discontinuity theory, one may hypothetically divide the recessed circular cylinder at Sections *A-A* and *B-B* into three free bodies, as shown in FIGURE 4. Free Body 1 is of wall thickness $t_1$ and is considered long enough so that it may be analyzed as a semi-infinite cylinder. Free Body 2 is of wall thickness $t_2$ and length $\ell_2$, whereas free body 3 is of wall thickness $t_3$ and length $\ell_3$. In the most general case, free bodies 2 and 3 may be analyzed as short cylinders, but in practice they are often short enough to be analyzed as circular cylindrical rings.

In general, the mean radii of the three free bodies are not equal. Assuming them equal, however, is useful in reducing the number of parameters encountered in the problem. This assumption does not introduce appreciable error as long as the ratios of wall thicknesses to the mean radii are sufficiently small for shell theory to apply. Assuming equal mean radii does not imply, however, that the eccentricity between the center lines of adjacent bodies may be neglected when the effect of axial forces is considered. Even small eccentricities will induce modest bending moments for axial forces of reasonable magnitude.

FIGURE 4 shows each of the free bodies that make up the composite vessel, subjected to the applied loads such as pressure $p$ and axial force $F$, as well as to the axial force $H$, shear force $Q$, and bending moment $M$.

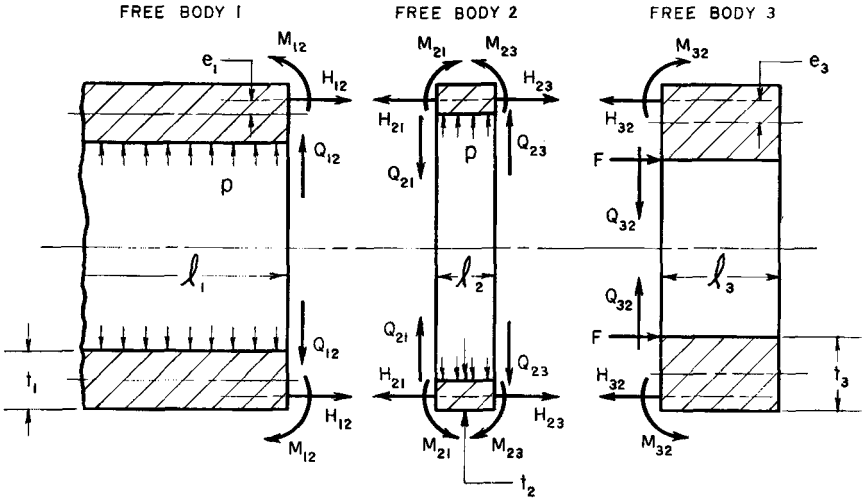


FIGURE 4. The free body diagrams of the recessed circular cylinder.

The resultant loads $H$, $Q$, and $M$ represent the stress system that existed at Sections *A-A* and *B-B* before the hypothetical cuts were made. The action of internal pressure in the axial direction at Sections *A-A* and *B-B* is not shown, however, since its effect is negligible and its introduction serves to unduly lengthen the over-all analysis. In order to distinguish the forces acting on Free Body 1 from those acting on Free Body 2, a double subscript notation is used; the subscript $ij$ indicates a force or moment on Free Body $i$ due to Free Body $j$.

It should be noted that the axial forces $H_{21}$ and $H_{23}$ are chosen to act at the mean radius of Free Body 2. Thus, the corresponding forces $H_{12}$ and $H_{32}$ are eccentrically located with respect to the mean radii of free bodies 1 and 3 by distances $e_1$ and $e_3$, respectively, where

$$e_1 = (t_1 - t_2)/2\,; \tag{25a}$$

$$e_3 = (t_3 - t_2)/2 \tag{25b}$$

All forces and moments in FIGURE 4 are shown so as to correspond with the sign convention previously established. Their actual directions will be indicated, of course, by the sign of the values obtained in the solution to the problem.

As discussed earlier, the resultant forces and bending moments at each junction initially are unknown quantities, but can be evaluated from continuity considerations. The associated set of equations may be found by application of the previously derived deformation equations to each of the free bodies.

As shown in FIGURE 4, the axial force $H_{12} = pR_1/2$, caused by the action of the internal pressure on the end closure, is not applied at the

mean radius of Free Body 1. This eccentric loading is due to the difference in the mean radii for the 2 adjacent bodies. Since the derivations presented in the previous sections were all based on the assumption that an axial force must pass through the mean radius of any cylinder, it is convenient to replace the eccentric load $H_{12}$ by an equivalent system of loading, consisting of force $H'_{12} = H_{12}$ acting at the mean radius and a bending moment $m_{12} = H_{12}\, e_1$ applied to the proper direction to account for the moment of $H_{12}$ about the axis at the mean radius. In view of EQUATIONS 25, the bending moment $m_{12}$ may also be expressed as

$$m_{12} = \frac{pR_1 t_1}{4}(1 - r) \tag{26}$$

where $r = t_2/t_1$.

In the analysis of Free Body 1, it is convenient to combine the moment due to the eccentric axial load with the pure bending moment $M_{12}$ and consider a net bending moment $M'_{12}$ where

$$M'_{12} = M_{12} - m_{12} \tag{27}$$

The net moment $M'_{12}$, as well as the axial force $H'_{12}$, act at the mean radius of Free Body 1. The deformations of Free Body 1, when considered a semi-infinite cylinder, may then be described according to EQUATIONS 23 as

$$w_{12} = -c\frac{\rho}{Et_1} M'_{12} - d\frac{\rho^{3/2}}{E} Q_{12} - (1 - \frac{\mu}{2})\frac{pR_1^2}{Et_1} \tag{28a}$$

$$\theta_{12} = a\frac{\rho^{1/2}}{E} M'_{12} + c\frac{\rho}{ET_1} Q_{12} \tag{28b}$$

where

$$\rho = R_1/t_1 \tag{29}$$

and where force $T$ in EQUATION 23 is zero since there is no external force acting on the cylinder. If the expressions for the bending moments given by EQUATIONS 26 and 27 are introduced into the deformations of EQUATIONS 28, they may be rewritten to read

$$w_{12} = -c\frac{\rho}{Et_1} M_{12} - d\frac{\rho^{3/2}}{E} Q_{12} + \frac{c}{4}\frac{p\rho}{E} R_1 (1 - r) - (1 - \frac{\mu}{2})\frac{pR_1^2}{Et_1} \tag{30a}$$

$$\theta_{12} = a\frac{\rho^{1/2}}{E} M_{12} + c\frac{\rho}{Et_1} Q_{12} - \frac{a}{4}\frac{p\rho R_1}{E}(1 - r) \tag{30b}$$

where bending moment $M_{12}$, of course, corresponds to the original one shown in FIGURE 4.

If one now multiplies the deflection equation by $\alpha$ and the rotation equation by $\gamma$ where

$$\alpha = E/\rho^2 pt_1 \; ; \quad \gamma = E/\rho^{3/2} p \tag{31}$$

and if one introduces a new set of dimensionless ratios

$$Z_1 = \frac{M_{12}}{\rho p t_1^2} \; ; \qquad Z_2 = \frac{Q_{12}}{\rho^{1/2} p t_1} \; ; \qquad Z_3 = \frac{M_{23}}{\rho p t_1^2} \; ; \qquad Z_4 = \frac{Q_{23}}{\rho^{1/2} p t_1} \tag{32}$$

then EQUATIONS 30 may be written

$$\alpha w_{12} = -cZ_1 - dZ_2 + (c/4)(1 - r) - (1 - \mu/2) \tag{33a}$$

$$\gamma \theta_{12} = aZ_1 + cZ_2 - (a/4)(1 - r) \tag{33b}$$

These expressions describe the deformation of Free Body 1 at Section *A-A*. They will be used later, together with similar sets of equations for free bodies 2 and 3.

The deformations of Free Body 2 are described in EQUATIONS 16, 17, 18, and 19 when the body is a short cylinder or circular cylindrical ring. When these equations are applied to Free Body 2, which has a thickness $t_2 = t_1$ and a mean radius $R_1$, one finds

$$\theta_{21} = -\frac{bS_2\rho^{1/2}}{Er^{5/2}t_1^2} M_{21} + \frac{cB_2\rho}{Er^2 t_1} Q_{21} + \frac{bY_2\rho^{1/2}}{Er^{5/2}t_1^2} M_{23} + \frac{cK_2\rho}{Er^2 t_1} Q_{23} \tag{34a}$$

$$w_{21} = -\frac{cB_2\rho}{Er^2 t_1} M_{21} + \frac{dL_2\rho^{3/2}}{Er^{3/2}} Q_{21} + \frac{cK_2\rho}{Er^2 t_1} M_{23} + \frac{dV_2\rho^{3/2}}{Er^{3/2}} Q_{23} - (1 - \frac{\mu}{2}) \frac{pR_1^2}{Ert_1} \tag{34b}$$

$$\theta_{23} = -\frac{bY_2\rho^{1/2}}{Er^{5/2}t_1} M_{21} + \frac{cK_2\rho}{Er^2 t_1} Q_{21} + \frac{bS_2\rho^{1/2}}{Er^{5/2}t_1^2} M_{23} + \frac{CB_2\rho}{Er^2 t_1} Q_{23} \tag{34c}$$

$$w_{23} = \frac{cK_2\rho}{Er^2 t_1} M_{21} - \frac{dV_2\rho^{3/2}}{Er^{3/2}} Q_{21} - \frac{cB_2\rho}{Er^2 t_1} M_{23} - \frac{dK_2\rho^{3/2}}{Er^{3/2}} Q_{23} - (1 - \frac{\mu}{2}) \frac{pR_1^2}{Ert_1} \tag{34d}$$

where $\rho$ is defined in EQUATION 29 as before. The subscript 2 appearing with the influence coefficients $K$, $B$, $S$, $Y$, $L$, and $V$ are used to distinguish them from another set of coefficients to be used when studying Free Body 3.

Again, by multiplying the deflection equations by $\alpha$ and the rotation equations by $\gamma$ as defined in EQUATIONS 31 and by introducing the dimensionless ratios of EQUATIONS 32, one may write the deformations of EQUATIONS 34 as

$$\gamma\theta_{21} = -(bS_2/r^{5/2})\,Z_1 + (cB_2/r^2)\,Z_2 + (bY_2/r^{5/2})\,Z_3 + (cK_2/r^2)\,Z_4 \quad (35a)$$

$$\alpha w_{21} = -(cB_2/r^2)\,Z_1 + (dL_2/r^{3/2})\,Z_2 + (cK_2/r^2)\,Z_3 + (dV_2/r^{3/2})\,Z_4 - (1/r)\,(1-\mu/2) \quad (35b)$$

$$\gamma\theta_{23} = -(bY_2/r^{5/2})\,Z_1 - (cK_2/r^2)\,Z_2 + (bS_2/r^{5/2})\,Z_3 + (cB_2/r^2)\,Z_4 \quad (35c)$$

$$\alpha w_{23} = (cK_2/r^2)\,Z_1 - (dV_2/r^{3/2})\,Z_2 + (cB_2/r^2)\,Z_3 - (dL_2/r^{3/2})\,Z_4 - (1/r)\,(1-\mu/2) \quad (35d)$$

Analyzing Free Body 3, one notes that the axial force $H_{32} = pR_1/2$ does not act at the mean radius of the body. In view of this eccentricity, one may proceed as for Free Body 1 and replace the eccentric force by $H'_{32} = H_{32}$ acting at the mean radius and a bending moment arising from the eccentricity. This bending moment, in view of EQUATION 25*b*, is given by

$$m_{32} = pR_1t_1\,(\lambda - r)/4 \quad (36)$$

where $\lambda = t_3/t_1$. Similarly, if the force $F$, due to the pressure acting on the closure, is assumed distributed around the inner edge of Free Body 3, it induces a bending moment on Free Body 3, whose magnitude is $n_{32} = F\lambda t_1/2$. These effects may be combined with the original moment $M_{32}$ to yield a net moment $M'_{32} = M_{32} - m_{32} - n_{32}$, which may now be rewritten

$$M'_{32} = M_{32} - pR_1t_1\,(2\lambda - r)/4 \quad (37)$$

Since $H_{32}$ and $F$ are of equal magnitude but act in opposite directions, the net axial load on Free Body 3 is zero. Furthermore, the body is not acted upon by internal pressure or loading at the right end. Consequently, in EQUATIONS 16, 17, 18, and 19, $T = H = p = M_R = Q_R = 0$, and the deformation expression for Free Body 3 may be rewritten

$$\theta_{32} = -(bS_3\rho^{1/2}/E\lambda^{5/2}t_1^2)\, M'_{32} + (cB_3\rho/E\lambda^2 t_1)\, Q_{32}$$
$$w_{32} = -(cB_3\rho/E\lambda^2 t_1)\, M'_{32} + (dL_3\rho^{3/2}/E\lambda^{3/2})\, Q_{32}$$
$$\theta_{3R} = -(bY_3\rho^{1/2}/E\lambda^{5/2}t_1^2)\, M'_{32} + (cK_3\rho/E\lambda^2 t_1)\, Q_{32} \qquad (38)$$
$$w_{3R} = (cK_3\rho/E\lambda^2 t_1)\, M'_{32} - (dV_3\rho^{3/2}/E\lambda^{3/2})\, Q_{32}$$

where $\rho$ is again equal to $R_1/t_1$. The subscript 3 on the influence coefficients $K$, $B$, $S$, $Y$, $L$, and $V$ indicate that they refer to Free Body 3.

Upon substituting the expressions for $M'_{32}$ given by EQUATION 37 into EQUATIONS 38 and multiplying the resulting deflection and rotation equations by $\alpha$ and $\gamma$, respectively, one obtains

$$\gamma\theta_{32} = -(bS_3/\lambda^{5/2})\, Z_3 + (cB_3/\lambda^2)\, Z_4 + bS_3\,(2\lambda - r)/4\lambda^{5/2}$$
$$\alpha w_{32} = -(cB_3/\lambda^2)\, Z_3 + (dL_3/\lambda^{3/2})\, Z_4 + cB_3\,(2\lambda - r)/4\lambda^2$$
$$\gamma\theta_{3R} = -(bY_3/\lambda^{5/2})\, Z_3 + (cK_3/\lambda^2)\, Z_4 + bY_3\,(2\lambda - r)/4\lambda^{5/2} \qquad (39)$$
$$\alpha w_{3R} = (cK_3/\lambda^2)\, Z_3 - (dV_3/\lambda^{3/2})\, Z_4 - cK_3\,(2\lambda - r)/4\lambda^2$$

where the dimensionless ratios $Z_3$ and $Z_4$ are those defined in EQUATIONS 32.

EQUATIONS 33, 35, and 39 describe the deformations of the three free bodies at their surfaces of separation. For continuity of deformation at a junction of free bodies, the displacement and rotation at the left of the junction must equal the displacement and rotation at the right of the junction. Thus, one may write the continuity expressions

$$\gamma\theta_{12} = \gamma\theta_{21};\quad \alpha w_{12} = \alpha w_{21};\quad \gamma\theta_{23} = \gamma\theta_{32};\quad \alpha w_{23} = \alpha w_{32} \qquad (40)$$

When EQUATIONS 33, 35, and 39 are substituted into EQUATIONS 40, four simultaneous equations are obtained

$$\begin{aligned}
&\text{I}\,Z_1 + \text{II}\,Z_2 + \text{III}\,Z_3 + \text{IV}\,Z_4 + \text{V} = 0\\
&\text{II}\,Z_1 + \text{VI}\,Z_2 + \text{VII}\,Z_3 + \text{VIII}\,Z_4 + \text{IX} = 0\\
&\text{III}\,Z_1 + \text{VII}\,Z_2 + \text{X}\,Z_3 + \text{XI}\,Z_4 + \text{XII} = 0\\
&\text{IV}\,Z_1 + \text{VIII}\,Z_2 + \text{XI}\,Z_3 + \text{XIII}\,Z_4 + \text{XIV} = 0
\end{aligned} \qquad (41)$$

from which the unknown resultant shear forces and bending moments may be found. The unknown quantities are proportional to the terms, $Z_1$, $Z_2$,

$Z_3$, and $Z_4$ according to EQUATIONS 32. The coefficients I through XIV, which appear in EQUATIONS 41, are defined as

$$\begin{aligned}
\text{I} &= -b[2 + (S_2/\tau^{5/2})] & \text{VIII} &= -dV_2/\tau^{3/2} \\
\text{II} &= -c[1 - (B_2/\tau^2)] & \text{IX} &= (c/4)(1-\tau) - (1-\mu/2)[1 - (1/\tau)] \\
\text{III} &= bY_2/\tau^{5/2} & \text{X} &= -b[(S_2/\tau^{5/2}) + (S_3/\lambda^{5/2})] \\
\text{IV} &= cK_2/\tau^2 & \text{XI} &= -c[(B_2/\tau^2) - (B_3/\lambda^2)] \\
\text{V} &= a(1-\tau)/4 & \text{XII} &= bS_3(2\lambda - \tau)/4\lambda^{5/2} \\
\text{VI} &= -d[1 + (L_2/\tau^{3/2})] & \text{XIII} &= -d[(L_2/\tau^{3/2}) + (L_3/\lambda^{3/2})] \\
\text{VII} &= -cK_2/\tau^2 & \text{XIV} &= -[cB_3(2\lambda - \tau)/4\lambda^2] - [f/\tau]
\end{aligned} \tag{42}$$

For a given design, the constants $a$, $b$, $c$, and $d$ are functions of only Poisson's ratio and have numerical values as shown in TABLE 2. The influence coefficients $K$, $B$, $S$, $Y$, $L$, and $V$ for free bodies 2 and 3 are functions of $\beta\ell$ for the bodies and may be found in TABLE 1 if the value of $\beta\ell$ lies within the range $0.5 \leq \beta\ell \leq 5.0$, or from EQUATIONS 21 if $\beta\ell < 0.5$. Thus, EQUATIONS 41 represent four simultaneous expressions from which the dimensionless ratios $Z_1$, $Z_2$, $Z_3$, and $Z_4$ may be evaluated. The numerical value of the deflection and rotation at a junction may be determined by introducing these ratios into either of the two equations that describe the deformations at this junction. The coefficients $\alpha$ and $\gamma$ appearing in front of $w$ and $\theta$ are given by EQUATIONS 31.

The resultant bending moments and shear forces, which may also be of interest in a subsequent stress calculation, can be found from EQUATIONS 32.

It may be observed that with the use of the sign convention established earlier, the coefficients of the $Z$ terms in EQUATIONS 41 form a matrix that is symmetrical with respect to the principal diagonal. This property may serve as an interim check in numerical computations.

Furthermore, it is now evident that the entire analysis of the problem is expressed in terms of only the dimensionless influence coefficients and the wall thickness ratios, thus permitting relatively simple and expedient solutions of a large class of problems.

### *The Semi-Infinite Rocket Recessed To Accomodate a Square Key*

The analysis of the previous section may be applied to rocket structures similar to the one shown in FIGURE 1 in order to evaluate the effect of

the portion of the wall that extends beyond the keyway on the stiffness of the structure. Specifically, this section of the paper is concerned with a special case of the problem that is often encountered in practice, namely, the case where the wall thickness is uniform and recessed to accommodate a key of square cross section. Thus for the special case

$$t_2 = t_1/2; \quad t_3 = t_1; \quad \ell_2 = t_1 \tag{43}$$

and

$$r = t_2/t_1 = 1/2; \quad \lambda = t_3/t_1 = 1 \tag{44}$$

To obtain an over-all view of the stiffening effect in this special case, numerical values are determined for the deformations at Section *B-B* in FIGURE 1 for various values of $(\beta\ell)_2$ and $(\beta\ell)_3$. These deformations may be used as a measure of the stiffness of the structure. The numerical value of $(\beta\ell)_2$, of course, is determined by the design of the keyway, and the numerical value of $(\beta\ell)_3$ is determined by the design of the reinforcing section, Free Body 3.

For the particular case in which Poisson's ratio $\mu$ is 0.3, $(\beta\ell)_2 = 0.5$ and $(\beta\ell)_3 = 0.2$, calcualtions reveal that $\gamma\theta_{32} = 6.315$ and $\alpha w_{32} = -2.305$. The results of other similar calculations for three different values of $(\beta\ell)_2$ and a range of $(\beta\ell)_3$ are depicted in FIGURE 5, which shows the dimensionless radial displacement $\alpha w_{32}$ plotted against $(\beta\ell)_3$. It can be seen that for a constant value of $(\beta\ell)_2$ the radial deflection decreases with an increase in length of Free Body 3. The rate of decrease is quite pronounced for $(\beta\ell)_3 < 1.0$, but diminishes rapidly until the effect of additional material becomes negligible for large values of $(\beta\ell)_3$. It may also be observed that the curves corresponding to $(\beta\ell)_2 = 0.2$, and 0.3 are indistinguishable from each other for the scale used. One would similarly expect to find that the curves for $(\beta\ell)_2 < 0.2$ do not differ markedly from those for $(\beta\ell)_2 = 0.3$.

Examination of the curves of FIGURE 5 further reveals that there does exist an optimum design, at which the addition of more material does not produce a noticeable increase in the rigidity of the structure (addition of material does, of course, add to the over-all weight). In general, this optimum design occurs for $1.0 < (\beta\ell)_3 < 2.0$. Since the maximum rigidity of the structure is essentially attained at $(\beta\ell)_3 = 1.0$, this single condition may be selected, for the sake of simplicity, as representative of the optimum condition.

A similar set of computations for the dimensionless rotation $\gamma\theta_{32}$ leads to an identical conclusion.

For steel, for which Poisson's ratio is 0.3, the optimum length corresponding to $(\beta\ell)_3 = 1.0$ may be expressed, in view of EQUATIONS 2 and 44, as

$$\ell_{3\ \text{optimum}} = 0.778\sqrt{R_1 t_1} \tag{45}$$

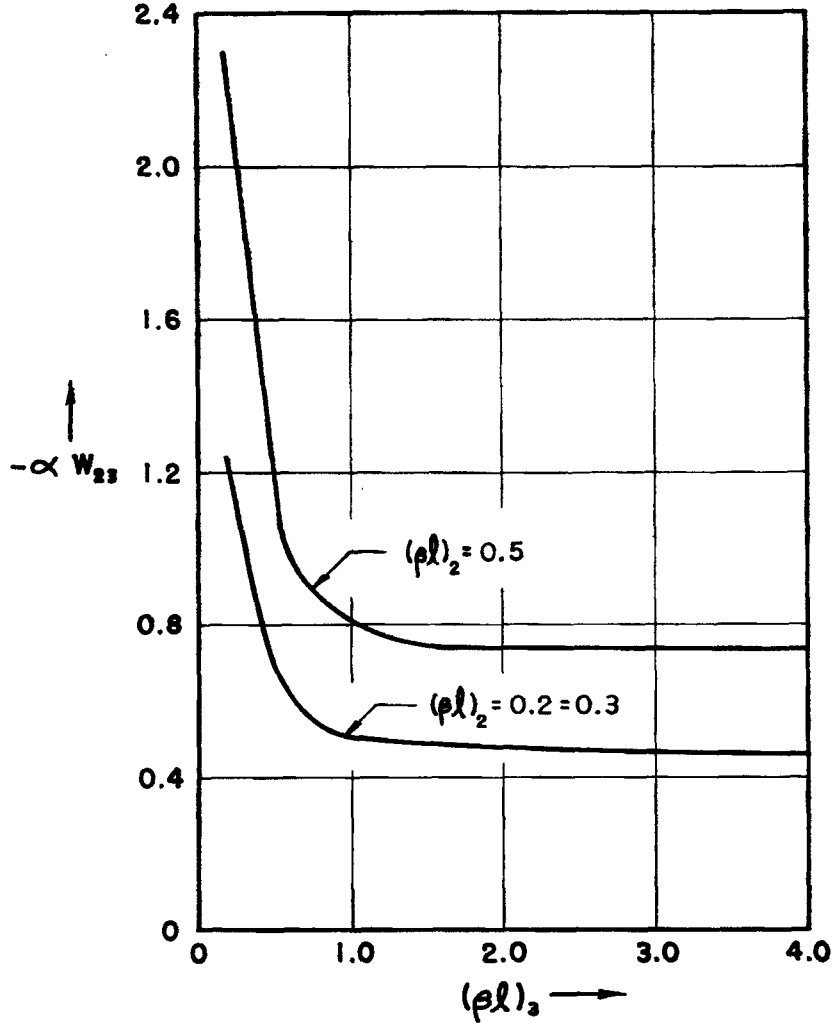


FIGURE 5. The radial displacement at section *BB*.

This simple relationship may be employed in design to obtain a structure of maximum rigidity at minimum weight.

## *Concluding Remarks*

Analyses of the circular cylinder subjected to axially symmetrical loads have shown that it is possible to categorize the problem into three basic types: the circular cylindrical ring, the short circular cylinder, and the semi-infinite circular cylinder. In summary, a unit may be considered a circular cylindrical ring when its value of $\beta\ell < 0.5$, a short circular cylinder when $0.5 \leq \beta\ell \leq 5.0$, and a semi-infinite circular cylinder when

$\beta > 5.0$. The deformations of the ends of both the circular cylindrical ring and the short circular cylinder are given by EQUATIONS 16, 17, 18, and 19. The influence coefficients for the short cylinder are defined in EQUATIONS 9 and TABLE 1, while the coefficients for the circular cylindrical ring are given by EQUATIONS 21. The deformations in the semi-infinite case are given in EQUATIONS 23 and 24.

By applying a discontinuity type of analysis to the semi-infinite rocket containing a circumferential keyway, it was found that the cylindrical portion beyond the keyway behaves as a reinforcing ring. Furthermore, when the keyway is designed to accommodate a square key, the length of the protruding portion of the rocket wall should be designed according to EQUATION 45 in order to obtain maximum stiffness for minimum weight.

Although the latter results were based on a set of calculations for only three values of $(\beta\ell)_2$, the conclusions apply for most rocket designs. This fact becomes apparent upon investigation of the results associated with the smallest and largest values used. For example, it may be observed by re-examining FIGURE 5 that there is no significant difference between the curves corresponding to $(\beta\ell)_2 = 0.2$ and those corresponding to $(\beta\ell)_2 = 0.3$. Furthermore, even for the limiting case of $(\beta\ell)_2 = 0$, which corresponds to a semi-infinite cylinder without a notch, the results do not differ significantly from those obtained for $(\beta\ell)_2 = 0.3$. Thus, the curve for $(\beta\ell)_2 = 0.3$ may be considered the lower bound of a family of curves for different values of $(\beta\ell)_2$.

Additional computations indicate that the upper bound is closely approximated by the curve for $(\beta\ell)_2 = 0.5$. Not only is it unlikely that this value is exceeded in a practical design, but it also represents the thickest structure for which shell theory applies. The latter conclusion, although not immediately obvious, may be reached by rewriting EQUATION 2 as

$$(\beta^4\ell^4)_2 = 3(1-\mu^2)(\ell_2)^4 / R_1^2 r^2 t_1^2 \tag{46}$$

and then letting $\ell_2 = t_1$ and $r = 1/2$, so that

$$(\beta\ell)_2 = 1.818/\sqrt{\rho} \tag{47}$$

where $\rho = R_1/t_1$. The numerical value of $(\beta\ell)_2 = 0.5$ corresponds to $\rho = 13.21$. Since shell theory applies only for $\rho > 10$, and it has been the foundation for the entire study, obviously this study would have little meaning for $\rho < 10$.

In developing the simple criteria established in this paper, attention was given only to the deformation problem and not to the associated stress problem. It is suggested that the latter effect be considered as a separate problem after establishing a given design with the optimum length as prescribed in EQUATION 45.

It may be remarked also that the manner in which discontinuity theory was applied to the axially symmetrical shell problem may be useful in solving other problems in the rocket or pressure vessel fields.

## *Summary*

The relationships between a system of axially symmetric loads applied to a thin circular cylinder and the resulting deformations were presented in a form particularly adaptable to numerical calculations. These relationships were applied to the problem of a semi-infinite rocket wall, containing a circumferential keyway and subjected to internal pressure. A simple design formula was derived that specifies the length of cylinder from the keyway to the end of the rocket needed to obtain maximum stiffness in the structure while making most economical use of the material.

## *Acknowledgment*

We thank A. R. Barzelay and E. P. Gebhard of the M. W. Kellogg Company, Jersey City, N. J., for permission to use some of the data on cylinders contained in an earlier report. The advantages of these data became apparent to us in the course of a research project conducted at New York University under a subcontract with the M. W. Kellogg Company, issued under Contract NOrd-12351, with the Department of the Navy, Bureau of Ordnance, Washington, D.C.

## *References*

1. WATTS, G. W. & H. A. LANG. 1952. The stresses in a pressure vessel with a flat head closure. Trans. ASME. 74(6): 1083-1090.
2. WATTS, G. W. & W. R. BURROWS. 1949. The basic elastic theory of vessel heads under internal pressure. J. Appl. Mechanics. 16(1): 55-73.
3. MCCALLEY, R. B. & R. G. KELLY. 1956. Tables of functions for short cylindrical shells. Paper No. 56-F-5. ASME.
4. HORVAY, G. & I. M. CLAUSEN. 1954. Stresses and deformations of flanged shells. J. Appl. Mechanics. 22(2): 109-116.
5. HORVAY, G. & I. M. CLAUSEN. 1955. Membrane and bending analysis of axisymmetrically loaded axisymmetrical shells. J. Appl. Mechanics. 22(1): 25-30.
6. TIMOSHENKO, S. 1940. Theory of Plates and Shells. McGraw-Hill, New York, N. Y.
7. MAYER, E., S. R. SADIN & H. V. WALDINGER. 1952. Stresses and deformations in thin shells of rotational symmetry with application to rocket walls. Approved by A. R. Barzelay, F. V. Walsh, & A. Kalitinsky. Proprietary Research and Development Rept. SPD 340. Prepared by M. W. Kellogg Co. Spec. Projects Dept. Jersey City, N. J. for Dept. of Navy, Bureau of Ordnance. Contract No. NOrd-12351. Washington, D. C.